Ocean Modelling 94 (2015) 141–152

Contents lists available at ScienceDirect

Ocean Modelling

journal homepage: www.elsevier.com/locate/ocemod

Model sensitivity of the Weddell and Ross seas, Antarctica, to vertical mixing and freshwater forcing

Joakim Kjellsson[a,*], Paul R. Holland[a], Gareth J. Marshall[a], Pierre Mathiot[a], Yevgeny Aksenov[b], Andrew C. Coward[b], Sheldon Bacon[b], Alex P. Megann[b], Jeff Ridley[c]

[a] British Antarctic Survey, Cambridge, UK
[b] National Oceanography Centre, Southampton, UK
[c] MetOffice, Exeter, UK

ARTICLE INFO

Article history:
Received 1 April 2015
Revised 15 August 2015
Accepted 19 August 2015
Available online 28 August 2015

Keywords:
Weddell sea
Ross sea
NEMO
CICE
Convection
Sea ice

ABSTRACT

We examine the sensitivity of the Weddell and Ross seas to vertical mixing and surface freshwater forcing using an ocean–sea ice model. The high latitude Southern Ocean is very weakly stratified, with a winter salinity difference across the pycnocline of only ~0.2 PSU. We find that insufficient vertical mixing, freshwater supply from the Antarctic Ice Sheet, or initial sea ice causes a high salinity bias in the mixed layer which erodes the stratification and causes excessive deep convection. This leads to vertical homogenisation of the Weddell and Ross seas, opening of polynyas in the sea ice and unrealistic spin-up of the subpolar gyres and Antarctic Circumpolar Current. The model freshwater budget shows that a ~30% error in any component can destratify the ocean in about a decade. We find that freshwater forcing in the model should be sufficient along the Antarctic coastline to balance a salinity bias caused by dense coastal water that is unable to sink to the deep ocean. We also show that a low initial sea ice area introduces a salinity bias in the marginal ice zone. We demonstrate that vertical mixing, freshwater forcing and initial sea ice conditions need to be constrained simultaneously to reproduce the Southern Ocean hydrography, circulation and sea ice in a model. As an example, insufficient vertical mixing will cause excessive convection in the Weddell and Ross seas even in the presence of large surface freshwater forcing and initial sea ice cover.

1. Introduction

The Southern Ocean plays an important role in the climate system. It is the world's only circumpolar ocean where the Indian, Pacific and Atlantic oceans exchange water masses and, together with the North Atlantic, is the source for one of the world ocean's two types of deep water. It is of importance for the global ocean circulation and the coupled atmosphere–ocean heat, freshwater and carbon cycles. Realistic simulations of the present climate and reliable projections of future climates are thus dependent on the fidelity of modelled processes in the high southern latitudes.

Observational data, although sparse, show summers with a warm and fresh mixed layer on top of cold and saline winter water (WW), the remnant of the deep winter mixed layer (cf. Timmermann and Beckmann, 2004). In turn, WW overlies a warmer and saltier Circumpolar Deep Water (CDW) at ~500 m depth and cold, salty Antarctic Bottom Water (AABW) in the deep ocean. In winter, the surface cools to freezing temperature and sea ice forms, increasing the salinity in the mixed layer due to brine rejection. Since density is mostly a function of salinity at near-freezing temperatures, the weak vertical salinity gradient results in generally weak stratification, especially in winter.

Coupled climate models tend to reproduce the hydrography, circulation and sea ice of the Southern Ocean poorly (Heuzé et al., 2013; Meijers, 2014; Turner et al., 2012). The complex atmosphere–sea-ice–ocean–ice-sheet interactions governing Southern Ocean salinity are seldom well-represented in global climate models. For example, they often fail to produce AABW correctly by spilling dense water off the continental shelf, forming AABW instead by unrealistic open-ocean convection (Heuzé et al., 2013). They also tend to underestimate the mixed layer depth thus overestimating the summer sea surface temperature (SST) in the open ocean (Meijers, 2014; Sallée et al., 2013; Wang et al., 2014), and fail to reproduce the observed mean state or trends of Antarctic sea ice (Turner et al., 2012).

* Corresponding author. Tel.: +441223221651.
E-mail address: tomkje@bas.ac.uk, joakimkjellsson@gmail.com, j.kjellsson@bas.ac.uk (J. Kjellsson).

http://dx.doi.org/10.1016/j.ocemod.2015.08.003
1463-5003/

One very common problem is the presence of deep open-ocean convection and associated sea ice polynyas, i.e. sea ice free areas in the sea ice pack. Unrealistic winter polynyas lead to altered hydrography, and unrealistically strong subpolar gyres in winter (Heuzé et al., 2013; Stössel et al., 2015; Timmermann and Beckmann, 2004; Timmermann and Losch, 2005). Studies using ocean–sea-ice models have indicated that vertical mixing must be sufficiently high to reproduce the mixed layer depth and alleviate this problem (Goosse et al., 1999; Heuzé et al., 2015; Stössel et al., 2007; Timmermann and Beckmann, 2004). Sallée et al. (2013) found that many coupled models underestimate the mixed-layer depth in the Southern Ocean, indicating insufficient vertical mixing. Studies have also indicated the importance of adding glacial meltwater from the Antarctic continent to the Southern Ocean to account for ice-shelf melting along the coast and icebergs melting in the open ocean (Häkkinen, 1995; Marsland and Wolff, 2001; Stössel et al., 2007). Insufficient vertical mixing or freshwater flux results in a salinity bias at the surface that will erode the weak stratification and cause deep convection. This brings heat and salt from the CDW into the mixed layer, so that polynyas open in the winter ice cover and further increase fluxes of heat and freshwater to the atmosphere, thus producing further convection. Such polynyas are very rare in our observational record and were only observed a few times in the mid- to late 1970s (Carsey, 1980; Comiso and Gordon, 1987) when satellite observations began. Model studies suggest that these events may be part of multi-decadal or centennial variations, where convection starts due to a build-up of CDW at depth and terminates when all CDW is depleted (Martin et al., 2013; Santoso and England, 2008). However, the validity of these findings depends on the ability of the model to reproduce the observed mean state of ocean, atmosphere and sea-ice well simultaneously, which is difficult in a coupled model (Heuzé et al., 2013; Hosking et al., 2013).

Simulations with large, unphysical polynyas and deep convection cannot be used for studying the past and future climates of Antarctica and the Southern Ocean, which is crucial to quantify and understand sea level rise, the carbon sink, and the observed expansion of Antarctic sea ice. We must thus understand where, when and why these polynyas and deep convection events occur. In this study we use an ocean–sea-ice model to assess the sensitivity of the high latitude Southern Ocean and its sea ice to freshwater forcing, vertical mixing parameters, and amount of initial sea ice. By using atmospheric data from reanalysis to force the ocean–sea-ice model we are able to constrain the results to observations better than in a fully coupled climate model. We will consider vertical mixing, freshwater forcing, and initial sea ice simultaneously, while previous studies have only focused on one of them (Heuzé et al., 2015; Marsland and Wolff, 2001; Stössel et al., 2015; Timmermann and Beckmann, 2004). We will show that insufficient surface freshwater forcing, vertical mixing, and initial sea ice can all have the same effect, i.e. allow for excessive deep convection in the Weddell and Ross seas, and we will discuss their common mechanism.

2. Methods

2.1. Data

We use the World Ocean Atlas 2013 (WOA13) gridded product (Locarnini et al., 2013; Zweng et al., 2013) to provide initial temperature and salinity for the ocean–sea-ice model described below and to validate the model results. Observations south of ~60 °S are sparse and biased towards summertime conditions, though the dataset does contain observations from Argo floats and tagged seals. Observations are somewhat concentrated along common supply ship routes, e.g. the prime meridian and the Antarctic Peninsula, and more data is available in the Weddell Sea than the Ross Sea. There are generally more observations of temperature than of salinity. Much of the gridded data in sea-ice covered regions are found by interpolation from the nearest available observations. Our knowledge of the ocean state below sea ice is thus very uncertain.

We also use observations of sea ice concentration from the Bootstrap data set, version 2 (Comiso, 2000), and estimated sea ice thickness from ICESat data (Kurtz and Markus, 2012). Both data sets are based on satellite data. Note that the ice thickness data are derived from observed freeboard using the assumption that all freeboard is snow and all draft is ice. Ice thickness data are not available for austral winter.

2.2. Model configuration

We use the NEMO (Nucleus for European Modelling of the Ocean) global general circulation model (Madec, 2014), version 3.6 revision 4672, coupled to the CICE sea-ice model, version 5.0.4 revision 801 (Hunke et al., 2013). NEMO and CICE are the ocean and sea-ice components of the HadGEM3 coupled climate model (Rae et al., 2014). Our model settings are similar to Megann et al. (2014) and Calvert and Siddorn (2013) except for the horizontal resolution, parameterisation of eddy-induced horizontal transport and vertical mixing parameterisation, as described below, and sea ice-ocean coupling which accounts for salt and mass exchanges between sea ice and ocean due to ice formation/melting (so called ice embedded option). Furthermore, the model is run without restoring surface salinity to climatological values. The model represents the global ocean using a tri-polar ORCA1 grid (Madec and Imbard, 1996) with nominal 1° horizontal resolution. South of 20 °S the model grid boxes are square, ranging from ~55 × 55 km at 60 °S to ~38 × 38 km at 70 °S. Eddy-induced transport is parameterised using a Gent–McWilliams (“GM”) scheme (Gent and McWilliams, 1990) with an iso-neutral tracer diffusion (Griffies et al., 1998) of maximum $A_{h,t} = 1000$ m^2 s^{-1} and horizontal momentum viscosity of maximum $A_{h,m} = 20000$ m^2 s^{-1}. These coefficients vary with grid box size so that $A_{h,t}$ and $A_{h,m}$ are about 1/2 of their maximum values at 60 °S. Vertical mixing is parameterised using a TKE scheme (Blanke and Delecluse, 1993; Gaspar et al., 1990), with a vertical eddy diffusivity coefficient, $c_k = 0.3$, which is higher than (Megann et al., 2014). The increased c_k is to have sufficient vertical mixing in the Southern Ocean, and the effects of using $c_k = 0.1$ as Megann et al. (2014) are discussed later. In addition, we use a parameterisation of breaking surface waves whereby an additional fraction, γ, of the surface TKE is added to the total TKE over an e-folding depth scale of H (cf. Calvert and Siddorn, 2013). In our reference simulation, $\gamma = 5\%$ and $H = 0.5$ m in the tropics, increasing to $H = 30$ m in mid-latitudes and polar regions. In the presence of sea ice, $\gamma = 0$. We also make use of tidal-induced vertical mixing from K1 and M2 tides, which is prescribed as a time-independent additional vertical mixing.

We force the model with ERA-Interim (Dee et al., 2011) liquid and solid precipitation, downwelling short- and long-wave radiation, 10 m zonal and meridional winds, 2 m air temperature and specific humidity, at 6 h ~0.7° horizontal resolution. ERA-Interim has been found to be the most reliable reanalysis for Antarctica and the Southern Ocean (Bracegirdle and Marshall, 2012; Bromwich et al., 2011). River runoff north of 60 °S is a monthly climatology from (Dai et al., 2009). South of 60 °S we vary the runoff between simulations. In our reference simulation we add a runoff of 2500 Gt yr^{-1} evenly distributed over the three grid boxes (~100 km) closest to the Antarctic coast to represent ice shelf melt, and 1500 Gt yr^{-1} in the rest of the Southern Ocean south of 60 °S to represent icebergs melting in the open ocean. These values are clearly higher than observed estimates from Rignot et al. (2013) and Silva et al. (2006) (~ 1300 Gt yr^{-1} from ice shelves and ~ 1100 Gt yr^{-1} from icebergs) as well as the estimates by Liu et al. (2015) (~ 1500 Gt yr^{-1} for ice shelves and ~ 760 Gt yr^{-1} from icebergs). Furthermore, the distribution of ice shelf and iceberg meltwater is very simple in the model, while the distribution in reality is more complex. We discuss the effect of the runoff later in the

Table 1
A list of the experiments in this study and the choice of parameters.

Experiment	Short description	R[Gt yr^{-1}]	c_k
REF	Reference	4000	0.3
MIX	Changed vertical mixing	4000	0.1
NO_INIT	No initial sea ice	4000	0.3
LOW_RNF	Low, evenly distributed runoff	2300	0.3
EVEN_RNF	Evenly distributed runoff	4000	0.3
SSR_RNF	Low, even runoff + correction	3759	0.3

paper, and present sensitivity simulations where both magnitude and distribution are changed.

For CICE, we use five ice thickness categories and five vertical layers (one for snow and four for ice). We use the recently developed "mushy" thermodynamics scheme (Turner et al., 2013) in which ice salinity and density, and thus conductivity, are tracers that evolve in space and time. This allows the ocean–sea-ice system to conserve salt. The time steps for both the thermodynamics and dynamics is 1 h, which is the same as in NEMO.

All simulations start in January 1979. We use the World Ocean Atlas 2013 (WOA13) monthly climatology gridded product (Locarnini et al., 2013; Zweng et al., 2013) to provide initial temperature and salinity for the ocean. The model will have initial sea ice where Bootstrap January 1979 sea ice concentrations exceed 15%, and model initial sea ice concentration is set to 100% and effective (grid-cell mean) thickness is set to 0.7 m. On top of the initial sea ice is also a 0.2 m thick snow layer (equivalent to 0.07 m ice). The initial sea ice is assumed completely fresh and the underlying ocean SST is set to freezing temperature. Sea ice area for January 1979 is $5 \cdot 10^6$ km^2 in the model and $4 \cdot 10^6$ km^2 in Bootstrap data. Averaged over the first summer, i.e. January–March 1979, the sea ice area is $2 \cdot 10^6$ km^2 in the model and $3 \cdot 10^6$ km^2 in Bootstrap data. This means that the model will have excessive melt in the first summer. However, this is offset by an initial positive salinity bias possibly caused by the model calculating a deeper mixed layer than in reality, therefore including some of the CDW in the mixed layer initially. Initial sea ice thickness of 0.7 m is close to the observed mean ice thickness by Kurtz and Markus (2012) and Worby et al. (2008) and that simulated by Holland et al. (2014). Sensitivity experiments show that the choice of initial sea ice thickness has a negligible effect on our final results if larger than ~0.7 m. Thinner initial sea ice results in a high salinity bias. We find that initialising the model with no sea ice introduces a salinity bias that can reduce the stratification enough to allow for open ocean deep convection.

2.3. Reference simulation

We run a series of sensitivity experiments using the NEMO/CICE configuration, all of which are listed in Table 1. The reference simulation, REF, uses the model configuration described above. All simulations start in 1979 and end in 2013, but similarly to Holland et al. (2014) we treat the period 1979–1992 as an initial spin up. However, we will analyse the spin-up period later on in the paper as results from the experiments diverge quite a lot during this time and polynyas often open up in the Weddell and Ross seas.

2.4. Mixing experiment

In the mixing experiment, MIX, we explore the sensitivity of the Southern Ocean and its sea ice to vertical mixing by adjusting the vertical eddy diffusivities and viscosities. The TKE closure scheme used to calculate vertical mixing (Gaspar et al., 1990) calculates the time-evolution of TKE using a one-dimensional equation that includes vertical eddy viscosity, K_m, and diffusivity, K_ρ (Madec, 2014). These two variables are in turn calculated by

$$K_m = c_k l_k \sqrt{\bar{e}}, \qquad K_\rho = K_m / \mathrm{P_r}, \tag{1}$$

where c_k is a tunable dimensionless coefficient, l_k is the dissipation length scale set by TKE and stratification, $\bar{e}$ is the TKE, and $\mathrm{P_r}$ is the Prandtl number. Increasing c_k will give more vertical mixing for a given amount of shear and stratification. We use $c_k = 0.3$ in the reference simulation and decrease to $c_k = 0.1$ in a reduced mixing simulation (MIX).

2.5. Initial sea ice experiment

In the initial sea ice experiment, NO_INIT, we start the model with no Antarctic sea ice. All other settings are identical to the reference simulation. Starting with no sea ice is commonly done in Southern Ocean models as they often start in January when the Antarctic sea ice extent is small. Examples include the experiments by Holland et al. (2014), Megann et al. (2014), and Timmermann and Beckmann (2004).

The initial sea ice used in the reference experiment is equivalent to about 0.7 m freshwater over the sea ice covered areas, which means that the NO_INT experiment will start with 0.7 m less freshwater over much of the marginal ice zone.

2.6. Freshwater forcing experiments

The runoff south of 60 °S used in the reference simulation is higher than observational estimates and concentrated along the Antarctic coast line. Note that our model does not explicitly simulate icebergs or ice shelves so that the meltwater from the Antarctic Ice Sheet and from icebergs must be prescribed as a "runoff" field. In two freshwater experiments, LOW_RNF and EVEN_RNF, we change the runoff south of 60 °S so that the runoff in m yr^{-1} is spatially constant, which is commonly done in ocean models. In LOW_RNF the total runoff is 2300 Gt yr^{-1} as the observed estimate by Rignot et al. (2013) and in EVEN_RNF it is 4000 Gt yr^{-1} as the reference simulation. In the last freshwater experiment, SSR_RNF, we use the runoff from LOW_RNF with an added correction. The correction is derived by running an experiment identical to LOW_RNF but where surface salinity is strongly restored towards the WOA13 climatology and the salt restoring correction is recorded. The time-mean of the salt restoring correction south of 60 °S is then added to the runoff field, acting as a static runoff with optimal spatial distribution. The total runoff in SSR_RNF is ~3800 Gt yr^{-1} of which ~850 Gt yr^{-1} is along the Antarctic coast and the rest in in the ocean south of 60 °S. The cǎcorrected" runoff comprises adding of freshwater along all of the Antarctic coastline except for along the eastern Antarctic Peninsula where freshwater is removed. This implies a positive salinity bias along the Antarctic coastline and a negative salinity bias along the Antarctic Peninsula when the runoff is 2300 Gt yr^{-1}.

3. Results

Some of our simulations exhibit excessive deep convection in the Weddell and Ross seas, so we focus our analysis on these two regions. We compare our model results to observations of ocean temperature and salinity from the WOA13-climatology (Locarnini et al., 2013; Zweng et al., 2013) and sea ice concentration and thickness from Bootstrap and ICESat data sets respectively (Comiso, 2000; Kurtz and Markus, 2012). As some of the main differences between experiments manifest during the spin-up periods, we will analyse the period 1979–1992 as well.

3.1. Reference simulation

Overall, the reference simulation reproduces the mean Southern Ocean surface and sea ice state well (Figs. 1, 2, 3). Sea surface tem-

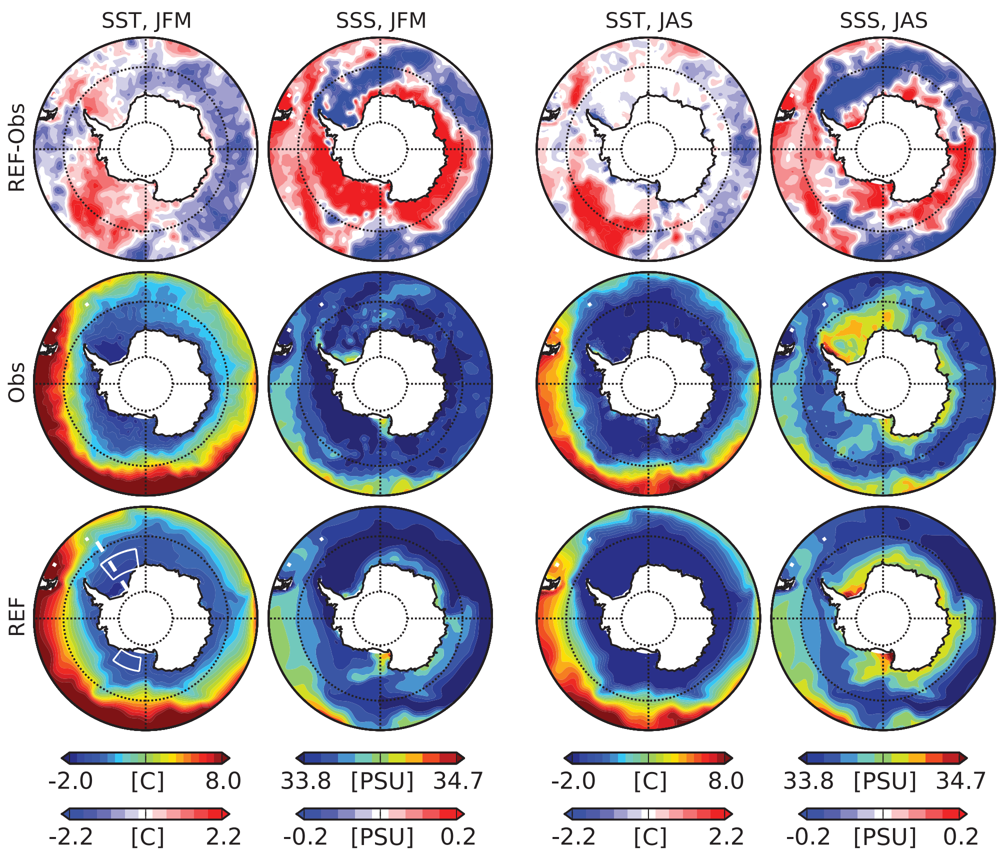

Fig. 1. Sea-surface temperature (SST) and sea-surface salinity (SSS) for austral summer (JFM) and winter (JAS) in observations from WOA13 climatology (middle row), reference simulation (bottom row), and the difference between the two (top row) averaged over 1992–2013. In the top row, or saltier than observations. White boxes in lower left figure show "Weddell" and "Ross" regions that are analysed in Figs. 5, 6, 7, 8, 10 and Table 2. White dashed line shows where a cross-section is taken for Fig. 4.

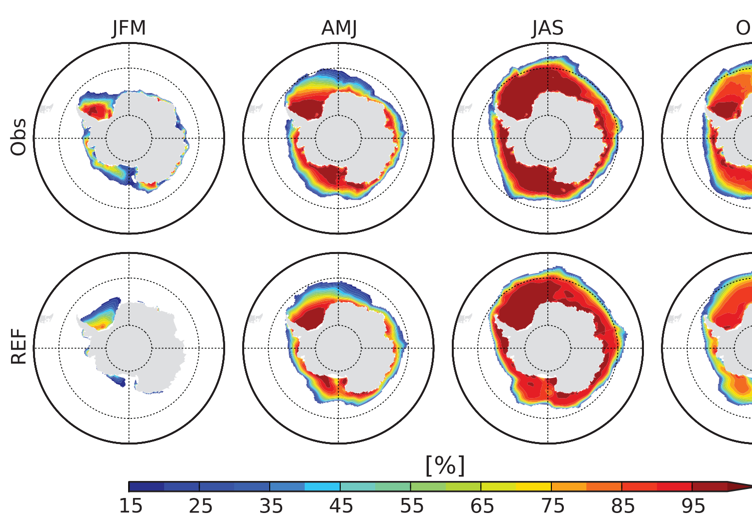

Fig. 2. Sea ice concentration for austral summer (JFM), autumn (AMJ), winter (JAS) and spring (OND) in observations (top row) and reference simulation (bottom row), both averaged over 1992–2013. Data is masked where ice concentration falls below 15%.

perature (SST) and salinity (SSS) are similar to the WOA13 climatology in both summer and winter (Fig. 1), although there is an overall positive salinity bias along the Antarctic coast except for east of the Antarctic Peninsula where there is a negative salinity bias. The bias along the coast is caused by the formation of high salinity shelf water (HSSW), and the bias east of the Antarctic Peninsula is likely caused by a deficit in sea ice formation. However, we stress that observations are extremely sparse in the winter season. In fact, observational studies have suggested that the salinity of HSSW is 34.7 PSU which is near the modelled salinity 34.5 PSU (Jacobs and Giulivi, 2010). The simulated summer sea ice concentrations are generally lower than the Bootstrap data, especially in the Ross (∼150 °W – 170 °E) and Amundsen seas (∼100 – 150 °W) (Fig. 2). Winter sea ice concentrations are almost as high as the observations, implying too much ice growth in autumn and too much melt in spring. It is possible that excessive near-surface salinity in the Ross Sea decreases the stratification and allows too much heat from the CDW to reach the surface which could explain the lack of summer sea ice.

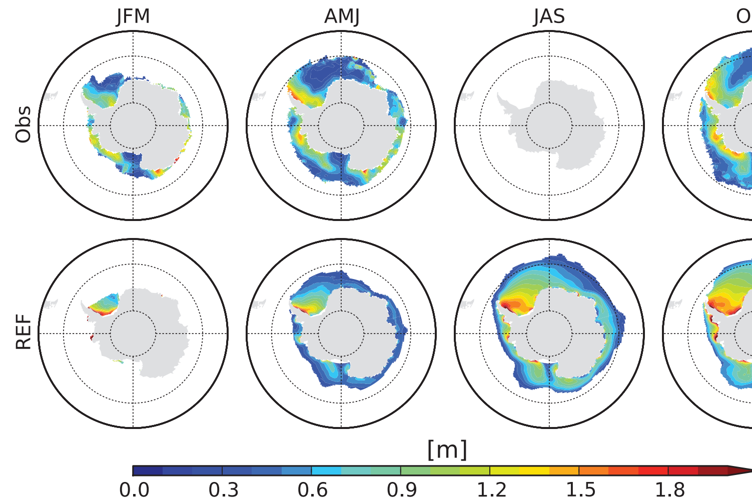

Fig. 3. Effective (grid-cell mean) sea ice thickness for austral summer (JFM), autumn (AMJ), winter (JAS) and spring (OND) in observations (top row) and reference simulation (bottom row) averaged over 1992–2013. Observations are unavailable in winter. Both observations and model data are masked where sea ice concentration is < 50%.

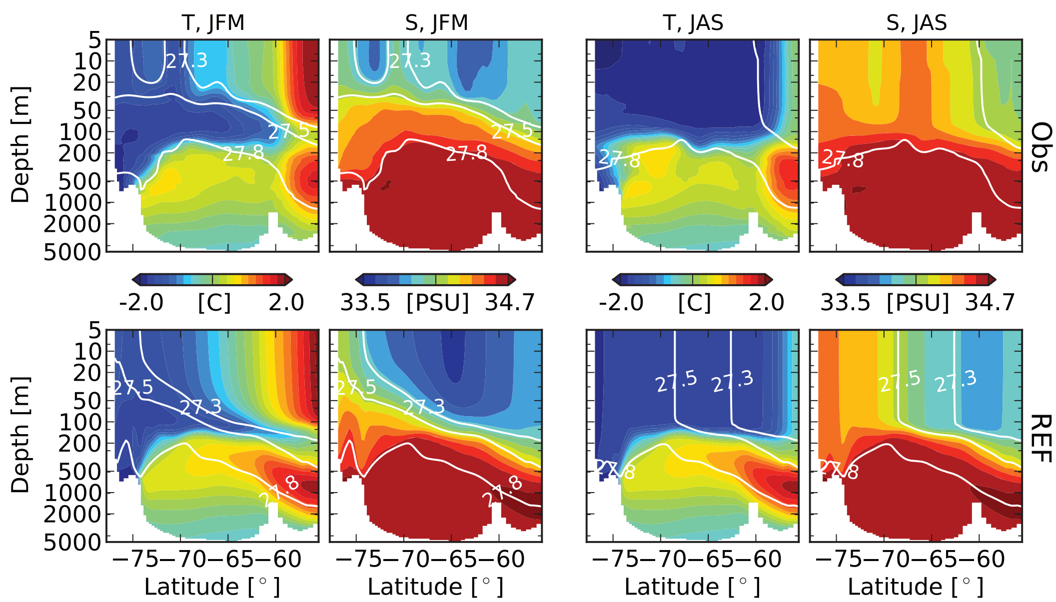

Fig. 4. Cross-section through the Weddell Sea (as indicated in Fig. 1) in observations (top row) and reference simulation averaged over 1992–2013. (bottom row). Left columns show T and S for austral summer (JFM) and right columns show T and S for winter (JAS). White lines show potential density referenced to surface, $\sigma_0 = 27.3, 27.5$, and 27.7 kg m^{-3}. Note the non-uniform depth axis.

The ice thickness is broadly correct, though too thick in most places, especially the Weddell Sea (Fig. 3) when compared to observations (Kurtz and Markus, 2012). However, since this data set uses the assumption that the freeboard is entirely snow, the data represent a lower bound for the actual ice thickness. The thick ice in the Weddell Sea and near the prime meridian may be due to an underestimation of vertical ocean heat fluxes over the Maud Rise seamount near 0 °E, 65 °S. In reality this seamount gives increased vertical heat fluxes and thus thinner sea ice, but this feature is not properly resolved in our simulation (Beckmann et al., 2001; Goosse and Fichefet, 2001; de Steur et al., 2007). Our model is forced with atmospheric reanalysis, where 2 m air temperature and humidity are highly influenced by the observed sea ice cover used as a surface boundary condition for the reanalysis model. We can thus expect to reproduce the sea ice extent fairly well, but ice thickness is a much less constrained variable that is more dependent on e.g. model physics (Holland et al., 2014; Massonnet et al., 2011). However, if the model simulates an area as ice free while it is ice covered in the ERA-Interim reanalysis, there will be open ocean with very dry air above which may lead to excessive evaporation and a salinity bias.

To examine the ocean model in a key region of spurious deep convection, we analyse a cross-section (78 °S to 55 °S) of the Weddell Sea in 1992, as indicated by the white dashed line in Fig. 1. The reference simulation reproduces the vertical temperature structure of the Weddell Sea well while the salinity is somewhat too fresh in the upper ~100 m, thus overestimating the stratification (Fig. 4). In general, the mixed layer is too fresh in all seasons, probably due to the high runoff in the reference simulation. However, we will show later in the paper that less runoff results in an unrealistic polynya in the Weddell Sea. Summer (JFM) is characterised by relatively warm and fresh water in a shallow mixed layer, and winter (JAS) is characterised by cold and salty water in a deeper mixed layer and weak stratification throughout the water column. Consequently, a layer of cold, salty WW remnant from the previous winter is found below the summer mixed layer. The situation is very similar in the Ross Sea. Timmermann and Beckmann (2004) found that the presence of this

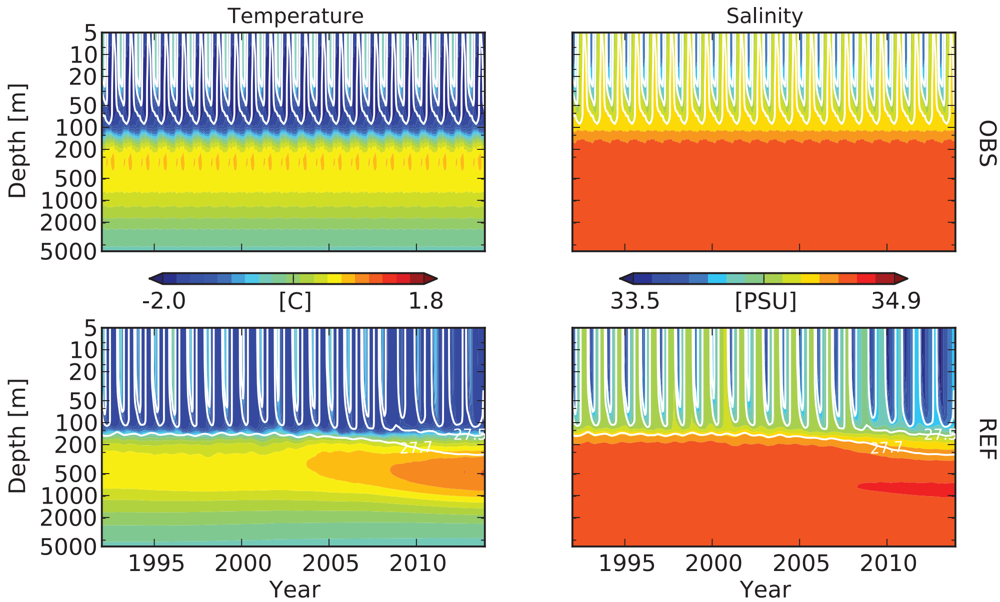

Fig. 5. Hovmöller plot of the mean temperature and salinity profiles in the Weddell Sea in WOA13 climatology and reference simulation. The WOA13 monthly climatology is repeated for the duration of the reference simulation for comparison. White lines show potential density referenced to the surface, $\sigma_0 = 27.3, 27.5$, and 27.7 kg m^{-3}.

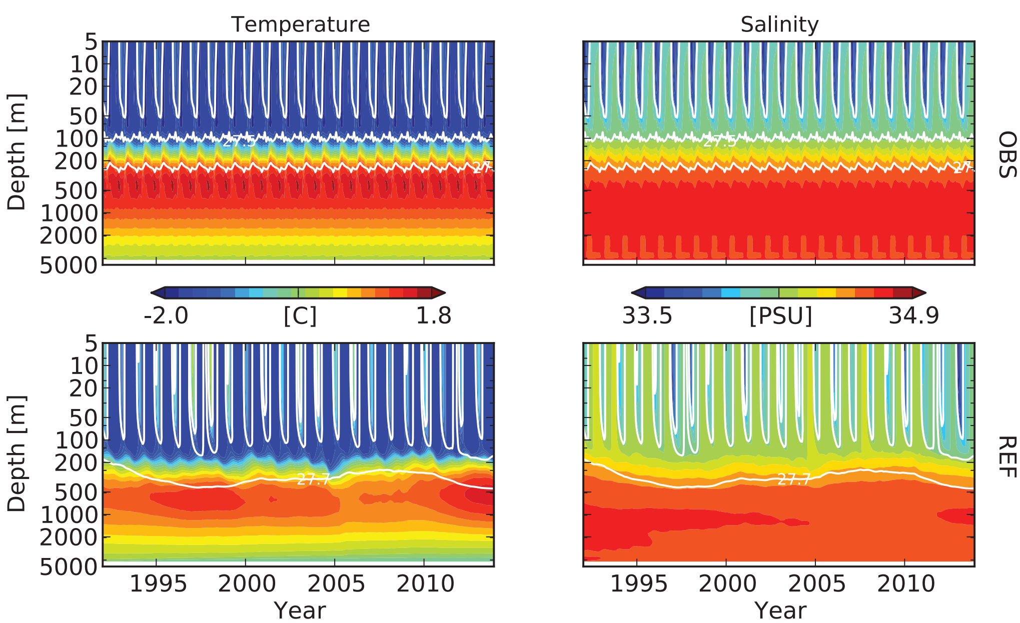

Fig. 6. Same as Fig. 5 but for the Ross Sea.

WW layer is sensitive to the choice of vertical mixing parameters and that it influences the occurrence of deep convection and polynyas in the central Weddell Sea. We discuss this further below. The reference simulation has a summer mixed-layer depth that is deeper than observations, as indicated by the depth of the $\sigma_0 = 27.3$ kg m^{-3} and $\sigma_0 = 27.5$ kg m^{-3} contours (Fig. 4), implying an overestimation of vertical mixing. Upper-ocean vertical mixing in the model is mostly set by surface stress and stratification. Overestimation of vertical mixing could therefore be due to overestimated surface stress, underestimated stratification or deficiencies with the parameterisations. In winter, the reference simulation shows salty water near the coast and fresher water to the north, a gradient not seen in the observations, although the quality of the observations beneath sea ice are highly questionable.

The temperature and salinity profiles of the Weddell and Ross seas (marked by white boxes in Fig. 1) agree fairly well with observations (Figs. 5, 6), although the model Weddell Sea has a somewhat fresher mixed layer than observations overall while the model Ross Sea is a little too saline. Both the model Weddell and Ross seas mixed layer freshen at the end of the simulation, which is discussed further below. Both regions show a seasonally varying upper ocean ($z < 200$ m) above a nearly constant deep ocean ($z > 200$ m). Both regions also simulate the weak stratification in winter but do not show signs of winter polynyas or open-ocean deep convection. We note that the Ross Sea is warmer and saltier at depth than the Weddell Sea in both observations and the reference simulation. In the mixed layer, however, the Ross Sea is colder and fresher than the Weddell Sea in observations but this feature is not seen in the simulation. However, we must stress that observations are sparse and that these observed differences may not be significant.

The surface freshwater forcing comprises four parts: evaporation (E), precipitation over open ocean (rain + snow, P_{tot}), runoff

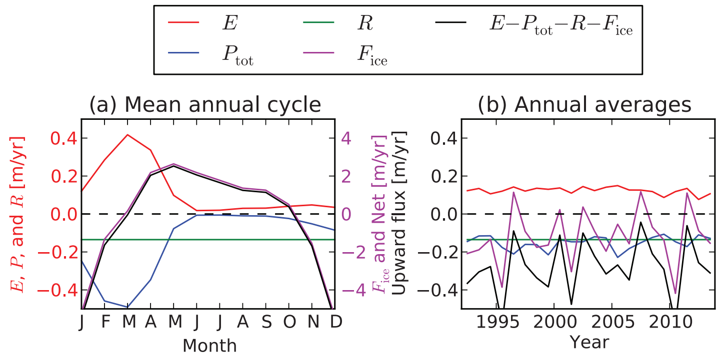

Fig. 7. Evaporation (red), precipitation (blue), runoff (green), sea ice freshwater flux (purple), and the net surface freshwater forcing (black) for the Weddell Sea in the reference simulation. Black dashed line shows the zero line. (a) Mean monthly values for each component. (b) Annual mean of each component. In a, the left vertical axis is for E, P and R, while the right vertical axis is for F_{ice} and the net, which are an order of magnitude larger. Units are $m\ yr^{-1}$. Positive corresponds to upward flux.(For interpretation of the references to colour in this figure legend, the reader is referred to the web version of this article)

Table 2
Annual mean evaporation, E, precipitation, P, runoff, R, and ice-ocean freshwater flux, F_{ice}, in the reference NEMO simulation 1992–2013. Weddell and Ross sea regions and the 60 °S latitude line are shown in Fig. 1. Positive indicates flux out of the ocean. All values in m yr^{-1}.

	E	P	R	F_{ice}	Total
Weddell	0.12	−0.15	−0.14	−0.12	−0.28
Ross	0.17	−0.16	−0.13	0.26	0.14
lat ≤ 60 °S	0.32	−0.47	−0.19	0.03	−0.32

(R), and total freshwater flux from sea-ice to ocean (F_{ice}). The latter, F_{ice}, includes freshwater fluxes due to sea ice growth/melt as well as evaporation, E_{ice}, and precipitation, P_{ice}, on sea ice. As $E_{ice} - P_{ice} < 0$ in general, $F_{ice} < 0$ on a global and annual average. In the Weddell Sea, F_{ice} dominates the other components by an order of magnitude on sub-annual time scales (Fig. 7a) due to large sea ice growth and melt. However, on annual and inter-annual time scales the components are of comparable magnitude (Fig. 7b). The inter-annual variation of F_{ice} is large while the other components are more stable. A similar result was found by Timmermann et al. (2001), and the same is true for the Ross Sea in our reference simulation (not shown). A key difference between the Weddell and Ross regions is that F_{ice} and the net forcing adds freshwater to the former and removes it from the latter (Table 2). This requires an oceanic freshwater transport out of the Weddell Sea region, and one into the Ross Sea region, for a steady annual mean salinity. However, it should be noted that the annual mean salinity is not stable in these regions. As E, P_{tot}, R, and F_{ice} are of comparable magnitudes a bias in any one of them could result in a significant surface salinity bias, destabilising the water column and causing spurious open-ocean deep convection (see below). Marsland and Wolff (2001) and Stössel et al. (2007) found that adding runoff in the high latitude Southern Ocean stabilised the water column and prevented convection.

We find a distinct freshening of the Weddell and Ross seas mixed layer towards the end of the simulation (Figs. 5, 6), with the freshening being largest in the Weddell Sea. We note that there is a sharp drop in F_{ice} in 2009–2010 which can explain the freshening of the Weddell Sea (Fig. 7b). We find that the sea ice concentration in the Weddell Sea is anomalously low in summer 2010, which would explain this F_{ice} anomaly. The surface freshening causes stratification to increase so that less heat and salt can mix up which causes the increase in temperature and salinity at depth. A similar analysis of the freshwater budget in the Ross Sea (not shown) shows that variations in salinity both at depth and surface are also due to large variations in F_{ice}. Unlike the Weddell Sea, the Ross Sea exhibits significant inter-annual variations in mixed-layer temperature and salinity during the simulation (Fig. 6).

The modelled SST and SSS in the Weddell Sea vary seasonally following a cycle in temperature–salinity (T, S) space that resembles that of the WOA13 climatology (Fig. 8a). Fig. 8b–g shows the SST and SSS for the spin-up phase 1979–1992 for all model experiments, which is the period where results start to diverge significantly. We note that observations in winter are uncertain. For example, observations show a sudden increase in SST in August which is likely to be an error. Maximum temperature ($T \approx -0.3$ °C) and minimum salinity ($S \approx 33.8$ PSU) are found in January–February when sea ice extent is minimum. The surface waters then cool in March–August to the freezing point and salinity increases as sea ice grows. Temperature minimum ($T \approx -1.8$ °C) and salinity maximum ($S \approx 34.4$ PSU) occurs in September when sea ice extent is maximum. Temperatures then increase and salinities decrease in October–December as sea ice melts. This seasonal cycle of the sea surface was observed in the model study by Döös et al. (2012) and dubbed the "cryosphere cell" by Groeskamp et al. (2014). The water at ~500 m depth, however, does not show such a cycle but instead remains constant at $T \approx$ 0.5 °C, $S \approx 34.6$ PSU throughout the year in both the observations and the reference simulation (Fig. 8a,b), indicating that this water is isolated from the surface. The surface water in September has a potential density of $\sigma_0 = 27.71$ kg m^{-3} while the CDW at 500 m depth has $\sigma_0 = 27.82$ kg m^{-3} (both indicated by red lines in Fig. 8), which is extremely close. It is thus clear that only a ~0.2 PSU salty bias at the surface would remove the stratification and allow the surface water to mix with the CDW, causing more convection. The situation is similar for the Ross Sea (not shown) where the reference simulation has a slight salty bias at the surface but not enough to remove the stratification (which is somewhat stronger than in the Weddell Sea). We show in Appendix A that a 0.2 PSU salinity bias is equivalent to a surface freshwater forcing perturbation of approximately 0.6 m if we assume a mixed layer depth of 100 m. Comparing with the freshwater components in Fig. 7 we estimate that a ~30% bias in any component could yield a salinity bias of 0.2 PSU after a decade. We note that Bromwich et al. (2011) found that precipitation can differ by more than 30% in the Southern Ocean between different reanalyses as well as different observational products.

3.2. Changing vertical mixing

The reduced mixing simulation, MIX, has low sea ice extent in summer (not shown) and winter and large wintertime polynyas, which indicates deep convection and ventilation of the CDW (Fig. 9c). We will therefore analyse the "spin-up" period, 1979–1992, to find when convection occurs. Reducing c_k results in a shallower mixed

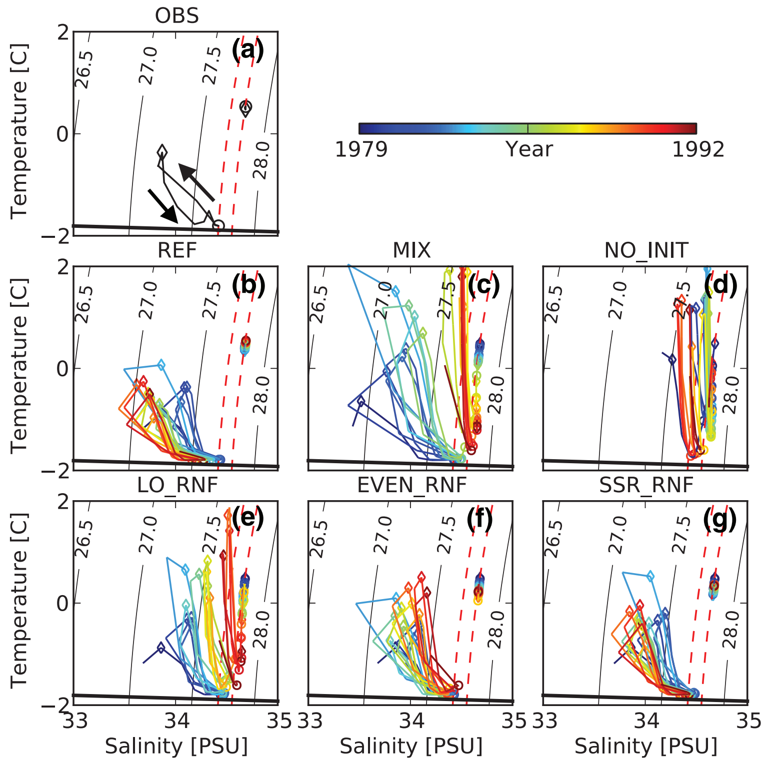

Fig. 8. Monthly averages of *T* and *S* at the surface and 500 m depth in the Weddell Sea for the years 1979–1992 for all runs listed in Table 1. February (warm, fresh) is shown by diamonds and September (cold, salty) by circles. Solid lines show potential density referenced to the surface, σ_0. Red dashed lines show the observed potential density at the surface and 500 m in September. Thick solid black line shows the freezing point of sea water.

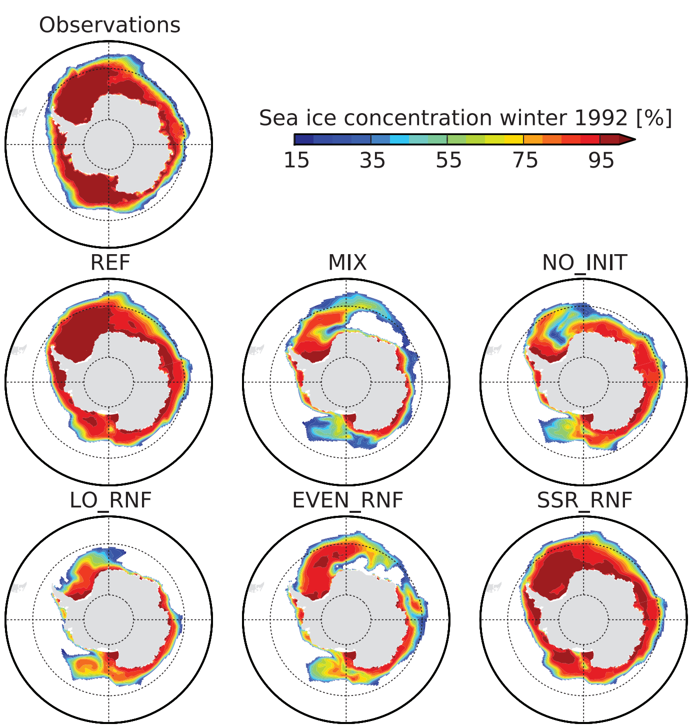

Fig. 9. Austral winter (JAS) sea ice concentration for all simulations listed in Table 1 averaged over 1992–1994.

layer depth in summer and winter for the first ~5 years (1979–1984; Fig. 10c) and winter mixed-layer salinity increases for each year (Fig. 8c). Winter sea ice extent increases somewhat during this period. In the sixth year of the MIX simulation, i.e. 1985, there is no layer

Table 3
Strength of the Weddell Gyre, Ross Gyre, and the ACC at Drake Passage in summer 1992 found by calculating a barotropic stream function from the model experiments. Observational estimates from Wang and Meredith (2008), Cunningham et al. (2003), and Chu and Fan (2007). Units in 1 Sv = 10^6 m^3 s^{-1}.

	Weddell gyre [Sv]	Ross gyre [Sv]	ACC [Sv]
OBS	56–97	20	134
REF	35	23	154
MIX	71	89	212
NO_INIT	85	92	212
LOW_RNF	36	73	220
EVEN_RNF	14	82	193
SSR_RNF	35	20	160

of winter water below the summer mixed layer in either the Weddell or Ross seas (not shown). The salinity in the winter mixed layer is close to that of the CDW below, and the stratification in winter is very weak. Deep convection then occurs for several consecutive winters (1986–1994) in both the Weddell and Ross gyres. It is clear that the surface water and CDW mix as they approach each other in *T*–*S* space (Fig. 8c). The surface temperature increase causes sea ice melt and large polynyas open in the Weddell and Ross seas (Fig. 9c). The increased SSS in the gyres produces increased horizontal density gradients, producing a Weddell Gyre of 71 Sv, a Ross Gyre of 89 Sv and an Antarctic Circumpolar Current (ACC) of 212 Sv by 1992, all larger than the reference simulation and than observational estimates (Table 3). Convection ceases in 1995 when all CDW is depleted. The simulated Weddell Sea starts to move towards a state where the SST is too high, the SSS is too low, and stratification is too strong. Intrusion of CDW at depth gradually increases temperature and salinity at ~500 m depth, but the bottom water remains too cold. The sea ice extent becomes larger than observations in winter and smaller than observations in summer.

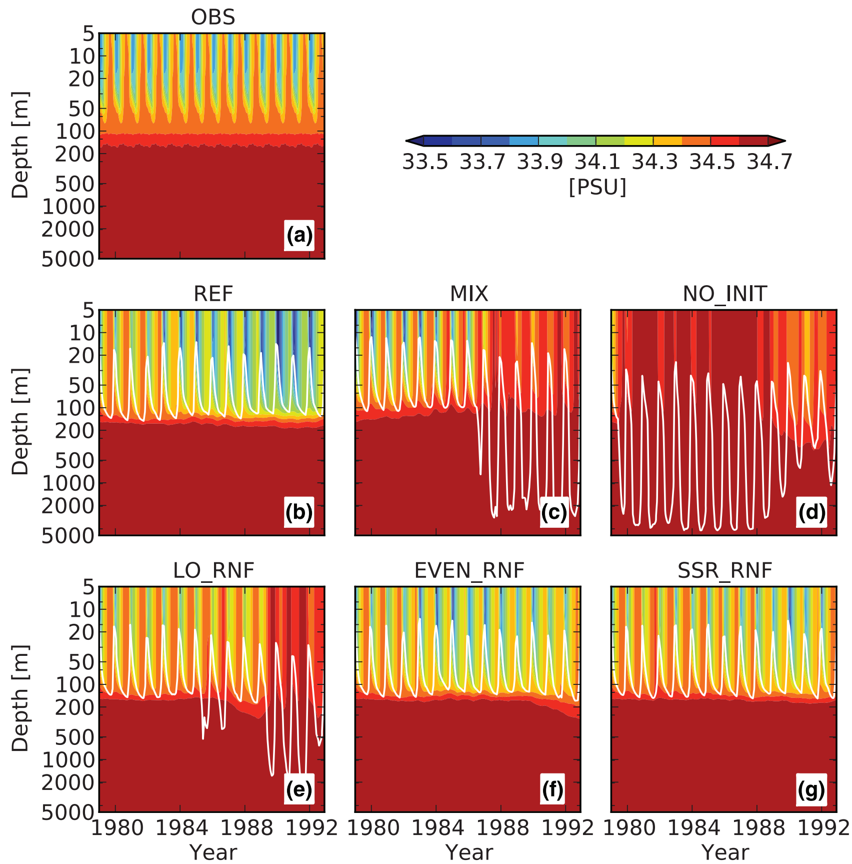

Fig. 10. Hovmöller plots of the mean salinity profile in the Weddell Sea for the years 1979–1992 of all simulations listed in Table 1. White lines show mixed layer depth from the model vertical mixing scheme.

Previous studies (Goosse et al., 1999; Haid and Timmermann, 2013; Stössel et al., 2007; Timmermann and Beckmann, 2004) have suggested that increasing vertical mixing in the Southern Ocean increases the downward transport of salt by distributing the freshwater in summer over a shallow mixed layer and the saltier water in winter over a deep mixed layer. This allows the model to maintain a weak but stable stratification in the Weddell and Ross seas throughout the simulation. It is clear that the same is true in our model, where the winter mixed-layer depth in the first 5 years is ~150m in the reference simulation and ~100m in the reduced mixing simulation.

3.3. Changing initial sea-ice condition

In our NO_INIT simulation a salinity bias develops immediately during the “spin-up” period 1979–1992 in the Weddell and Ross seas. This bias grows until the winter of 1980 (year 2 of the simulation) when the stratification is completely removed and the surface water mixes with the CDW (Figs. 10d, 8d). A small but clear Weddell Sea polynya can be found in the winter 1979, i.e. only six months into the simulation. Similarly to the MIX simulation, the increased surface temperature results in large polynyas in the Weddell and Ross seas (Fig. 9d). Also, the Weddell and Ross gyres and the ACC spin up to unrealistic strengths.

Compared to the reference simulation, the NO_INIT simulation has no ice cover in the first summer which allows for more heat to be absorbed by the mixed layer and for more evaporation which increases the SST and SSS (Figs. 8d, 10d). In the first summer, January–March 1979, the $E-P$ in the Weddell Sea is -0.1 m yr^{-1} in REF but -0.03 m yr^{-1} in NO_INIT. However, a much more important cause is that starting with no initial sea ice implies a freshwater deficit of ~0.7 m which is similar to the 0.6 m needed to produce a 0.2 PSU salinity bias. Analysis of the freshwater budget (not shown) shows that the reference simulation, which starts with 0.7 m thick ice (and another 0.07m of ice equivalent of snow) over much of the Weddell Sea, has ~0.6 m of melt in the first summer (January–March), while the surface salinity and sea ice area are close to observations. This is likely more than the melt occurring in reality. However, the excessive melt offsets an initial positive salinity bias possibly caused by the fact that the mixed layer depth is different in the model and observations so that some of the CDW is included in the model mixed layer initially. We also find that this melt comes from the initial sea ice in the region, and that the Weddell Sea is a net exporter of sea ice during the first year (< 0.01 m yr^{-1}). The NO_INIT experiment has no such melt initially and thus has a high salinity bias in the first summer that grows in autumn as sea ice grows. Another effect is that the salinity bias leads to weaker stratification, which eventually allows for mixing of surface water and CDW, thus further increasing the salinity bias. A close analysis of the mean profile in the Weddell Sea in the NO_INIT experiment shows that while salinity increases in the mixed layer, it also decreases below, indicating an upward transport of salt. We also find that the mixed layer is deeper in NO_INIT than in the reference experiment. The polynyas in the Weddell and Ross seas in the NO_INIT experiment can thus be explained by an initial freshwater deficit as well as an upward transport of salt. Increased evaporation seems to play a smaller role.

We speculate that the problem of excessive evaporation when summer sea ice extent is low could be reduced in coupled atmosphere–ocean–sea-ice simulations since increased evaporation would be reduced by increased 2 m specific humidity; in our reanalysis-forced ocean–sea-ice simulations there is no such feedback. It should also be noted that surface salinity biases due to insufficient initial sea ice are likely to be negligible if the model is integrated for a long time, e.g. ~100 years.

3.4. Changing freshwater forcing

Using the same settings as the reference simulation, we run three simulations where the magnitude and distribution of runoff from the Antarctic Ice Sheet is altered, LOW_RNF, EVEN_RNF, and SSR_RNF, as described earlier in the paper. The first two simulations, LOW_RNF and EVEN_RNF, show low sea ice extent in both summer and winter, with large wintertime polynyas in the Weddell and Ross seas, indicating deep convection and ventilation of the CDW (Fig. 9e,f). However, in EVEN_RNF the excessive convection does not fully reach into the Weddell Sea region so it remains stratified throughout the simulation (Fig. 10f). In the first few years of simulation (1979–1984), both simulations develop a high salinity bias along the Antarctic coast (not shown). It is likely that the initial salinity bias along the coast is due to coastal polynyas that create HSSW that in reality would, sink into the deep ocean but cannot in the present model configuration. This is partly due to the coarse resolution, and partly due to the choice of the vertical coordinate: it is well-known that z-level models struggle to accurately transport dense water down slopes (Doney and Hecht, 2002; Legg et al., 2006). We note that the freshwater forcing in LOW_RNF is evenly distributed while that observed by Rignot et al. (2013) is somewhat concentrated along the Antarctic coastline. However, experiments not shown here show that the results are almost identical when the both the magnitude and spatial distribution are as observed by Rignot et al. (2013). This coastal salinity bias spreads into the gyres and erodes the stratification. Analysis in *T*–*S* space shows that the surface water mixes with the CDW below (Fig. 8e,f) thus increasing surface temperature and salinity. As in the MIX simulation, the Weddell and Ross gyres and the ACC spin up to strengths larger than the reference simulation and than observations suggest (Table 3).

The third simulation, SSR_RNF, simulates the sea ice extent well and does not show signs of deep convection in the open ocean (Fig. 9g). The winter sea ice concentrations (Fig. 9g) and the Weddell Sea water masses in *T*–*S* space (Fig. 8g) look very similar to the reference simulation. The same is true for the Ross Sea. Furthermore, the gyre and ACC transports in SSR_RNF are similar to those in the reference simulation. It is interesting to note that the EVEN_RNF simulation shows deep convection occurring while the SSR_RNF does not, although the former has 200 Gt yr^{-1} more runoff. This shows that the presence of deep convection in the central Weddell and Ross Seas is sensitive to both the magnitude and spatial distribution of the runoff field. Further sensitivity experiments not included in this study indicate that runoff of less than 3800 Gt yr^{-1}, as in SSR_RNF, results in excessive convection and polynyas in the Weddell and Ross seas.

4. Discussion

Reducing the vertical eddy diffusivity, c_k, resulted in a homogenisation of the water column in the Weddell and Ross seas as the surface water mixed with the CDW, bringing heat and salt to the mixed layer and opening polynyas in the sea ice (Figs. 8,9,10). This result agrees with Goosse et al. (1999), Timmermann and Beckmann (2004), and Timmermann and Losch (2005) who suggested that modelling realistic hydrography and sea ice in the Weddell Sea requires sufficient vertical mixing in the top 100 m. Timmermann and Beckmann (2004) suggested a mechanism where insufficient vertical mixing allows salt from brine rejection to accumulate in the mixed layer and erode the stratification. The mixed layer salinity increases each year in our simulation, but it is also possible that this is due to the warm bias that gives a small summer sea ice cover and allows for increased evaporation. Summer evaporation in the MIX simulation in 1983 before deep convection occurs is 46% higher than in REF. Additional simulations (not shown) suggest that using the reduced vertical eddy diffusivity, $c_k = 0.1$, but adding a large fraction of the surface TKE, $\gamma = 50\%$, to the total TKE in the top ~30 m has a similar effect as using $c_k = 0.3$, as in the reference simulation. This confirms that it is vertical mixing near the surface that must be sufficient to stop convection and polynyas in our model.

We note that the presence of a Weddell Sea polynya in models appears to be very sensitive to the details of the mixing scheme. Megann et al. (2014) found that the changes made from the GO1 ocean configuration to GO5.0 overall led to improvements in the realism of the annual cycle of surface temperature and mixed layer depths. The GO5.0 has a newer version of NEMO where the TKE mixing scheme has been changed and tuned by Calvert and Siddorn (2013). However, in the “improved” GO5.0 model a large polynya nevertheless developed northeast of the Weddell Sea that was absent in the earlier configuration.

We demonstrated the sensitivity to surface freshwater forcing by altering the “runoff” from the Antarctic Ice Sheet. Previous studies have found that the surface freshwater forcing can control the presence of polynyas and deep convection in the high-latitude Southern Ocean (Goosse and Fichefet, 2001; Marsland and Wolff, 2001; Stössel et al., 2015). However, most of these studies concentrated on the magnitude of the freshwater flux. We also note that the model study by Holland et al. (2014) used a relatively high runoff to close the Weddell polynya, where 2000 Gt yr^{-1} was in the open ocean and some additional freshwater was added as ice shelf melt. We showed that the presence of deep convection and polynyas in the Weddell and Ross seas depends on both the magnitude and distribution of the runoff. Simulations where runoff is 2300 Gt yr^{-1} or 4000 Gt yr^{-1} evenly distributed over the Southern Ocean show excessive deep convection due to a salinity bias at the surface originating along the Antarctic coast. However, if the runoff is 4000 Gt yr^{-1} but concentrated along the Antarctic coast, as in the reference simulation, both the Weddell and Ross seas remain stratified and the sea ice cover agrees with observations. A recent study by Stössel et al. (2015) concluded that freshwater forcing must be small near the Antarctic coastline in order to produce dense water that can spill off the shelf break. Hence, if the model can produce AABW in a realistic fashion, a runoff of 4000 Gt yr^{-1} can greatly decrease the AABW production and lead to deficiencies in long (> 100 year) simulations.

Evaporation, precipitation, runoff and freshwater flux from ice growth/melt are found to be of similar magnitude on annual time scales. The salinity difference between WW and CDW is only 0.2 PSU, which can be eroded in a decade by a 30% bias in any of the freshwater fluxes. Thus, uncertainties in reanalysis precipitation (Bromwich et al., 2011), the sea-ice export (Uotila et al., 2014), or glacial melt (Rignot et al., 2013) can result in a salinity bias at the surface that erodes the stratification, causing excessive deep convection in the Weddell and Ross gyres. Our model does not include ice shelf cavities, which could lead to an underestimation of the freshwater forcing focussed along the Antarctic coast. We speculate that the freshwater forcing along the coast must be large enough to offset a model salinity bias created by coastal polynyas forming salty, dense water that is unable to sink into the deep ocean. Heuzé et al. (2013) show that none of the coupled climate models in their study form bottom water by spilling dense water off the shelf into the deep ocean, and several of the models instead form deep water by convection in the open ocean. This problem could possibly be circumvented by parameterising tunnels from the shelf into the deep ocean or artificially altering the bathymetry in the region, which is done in most models. Additional simulations (not shown) suggest that using such tunnels and increasing the advection through them is not enough to remove the salty bias along the Antarctic coast line in our model. We note that Stössel et al. (2007) showed that the coastal polynyas can be reduced by cooling water in contact with ice shelves at depth.

We demonstrated the sensitivity to initial sea ice conditions by starting a simulation with no sea ice. This is common modelling practice, but implies an initial freshwater deficit of the system. The magnitude of the deficit can be approximated as the mean ice thickness from observations, which is ∼0.7 m (Kurtz and Markus, 2012). This deficit in the first summer creates salinity biases in the Weddell and Ross seas that quickly erode the stratification, and allows salt to mix up from below. This results in polynyas in the Weddell and Ross seas, deep convection in the gyres and unrealistic spin-up of the ACC, similar to the results by Timmermann and Beckmann (2004) and Heuzé et al. (2015). This implies that underestimation of the initial sea ice extent could lead to excessive deep convection in models if the surface freshwater flux into the ocean is insufficient. A weak correspondence between low summer sea ice extent and open ocean deep convection was noted in coupled-model simulations in the CMIP5 archive (Heuzé et al., 2013). It could be because low summer sea ice implies more evaporation, both since more water is ice free but also because the SST becomes higher. More evaporation could cause a salinity bias at the surface and weaker stratification. However, Stössel et al. (2015) found that a coupled atmosphere–ocean–sea-ice model was able to better reproduce the observed Southern Ocean state than an ocean–sea-ice model forced by atmospheric reanalysis. This is because coupled models couple evaporation to near-surface specific humidity and precipitation so that the effect of overestimated evaporation can be greatly reduced. This implies that forced ocean–sea-ice models are more sensitive to the initial sea ice conditions and summer sea ice extent than coupled models.

We note that some modelling studies (Holland et al., 2014; Megann et al., 2014; Timmermann and Beckmann, 2004) do not use initial sea ice and do not see a Weddell Sea polynya. However, we stress that the results may very well vary between models due to variations in e.g. parameterisations, resolution and initial conditions.

It is likely that using a higher horizontal resolution would yield more realistic representation of the horizontal ocean circulation in the Weddell and Ross seas and on the shelf where dense water forms, although it is also likely that the AABW production is more dependent on the choice of vertical coordinate and vertical resolution (Legg et al., 2006). Mathiot et al. (2011) showed that the Antarctic Slope Current, which is important for sea ice drift and transport of water masses to and from the continental shelf, can only be properly resolved when horizontal resolution is 0.5° or finer. It is also possible that the resolution of the atmospheric reanalysis has an impact as the narrow and steep Antarctic Peninsula is often poorly resolved and since coastal polynyas depend on katabatic winds from the Antarctic continent. It is, however, beyond the scope of this study to investigate the effects of changing horizontal resolution of the ocean and/or atmosphere.

5. Conclusions

By altering the vertical eddy diffusivity, freshwater forcing and initial sea-ice conditions separately we have shown that errors in any one of them can cause excessive deep convection and sea-ice polynyas in models of the Southern Ocean. Our results also imply that the presence of deep convection and polynyas can only be controlled by considering all three factors simultaneously. As an example, deep convection occurred in the Weddell and Ross seas in the EVEN_RNF simulation due to the lack of freshwater forcing along the Antarctic coast despite the increased vertical mixing and relatively high total runoff in the Southern Ocean.

We show that the winter salinity difference between the mixed layer and the CDW at depth is only 0.2 PSU. Since the components of the surface freshwater forcing are of similar magnitude, ~ 0.2 m yr^{-1}, a ∼30% bias in any one of them can erode the stratification in about a decade. We also find that simulations with no initial sea ice start with a freshwater deficit that is enough to remove the stratification.

Many of the coupled-model simulations in the CMIP5 archive suffer from significant biases in the Southern Ocean, e.g. SST, SSS, mixed layer depth, sea ice extent etc., and many of them show signs of excessive open ocean deep convection (Heuzé et al., 2013; Meijers, 2014; Turner et al., 2012). Our sensitivity experiments indicate that this could be due to insufficient vertical mixing, summer sea ice or freshwater forcing, and it is clear that these biases must be considered together.

Acknowledgements

We wish to thank the two anonymous reviewers whose comments helped us improve the paper. This work was carried out as part of the UK Natural Environment Research Council grant NE/K012150/1: “Poles apart: why has Antarctic sea ice increased, and why can’t coupled climate models reproduce observations?”. We thank Adrian K. Turner for help with CICE, and Laurent Brodeau and Tim Graham for help with NEMO. We also thank Celine Heuzé for fruitful discussions. ERA-Interim forcing obtained from ECMWF with help from Tony Phillips. All simulations performed on the ARCHER UK National Supercomputing Service (http://www.archer.ac.uk) and we acknowledge the helpdesk for assistance.

Appendix A. Salinity change due to added/removed freshwater

We calculate the change in freshwater flux needed to produce a given change in salinity. We assume a mixed layer of 1 m^2 area and $H = 100$ m depth. Salinity is $S_1 = 35$ PSU and density is $\rho_1 = 1030$ kg m^{-3}. We then add Δz of freshwater, i.e. precipitation, which has density $\rho_0 = 1000$ kg m^{-3}. Let the new density and salinity be ρ_2 and $S_2 = S_1 + \Delta S$. For the new water column conservation of mass yields,

$$(H + \Delta z)\rho_2 = H\rho_1 + \Delta z \rho_0, \quad (A.1)$$

while salt conservation yields

$$(H + \Delta z)\rho_2 (S_1 + \Delta S) = H\rho_1 S_1. \quad (A.2)$$

Combing the two equations and solving for Δz we get

$$\Delta z = -\frac{H\rho_1 \Delta S}{\rho_0 (S_1 + \Delta S)}, \quad (A.3)$$

so to freshen a mixed layer by $\Delta S = 0.2$ PSU we would need to add $\Delta z \approx -0.6$ m freshwater. We note that the Δz freshwater required to provide and ΔS freshening scales linearly with the assumed mixed-layer depth, H.

References

Beckmann, A., Timmermann, R., Pereira, A.F., Mohn, C., 2001. The effect of flow at Maud Rise on the sea-ice cover - numerical experiments. Ocean Dyn. 52, 11–25.

Blanke, B., Delecluse, P., 1993. Low frequency variability of the tropical Atlantic Ocean simulated by a general circulation model with mixed layer physics. J. Phys. Oceanogr. 23, 1363–1388.

Bracegirdle, T.J., Marshall, G.J., 2012. The reliability of Antarctic tropospheric pressure and temperature in the latest global reanalyses. J. Clim. 25, 7138–7146.

Bromwich, D.H., Nicolas, J.P., Monaghan, A.J., 2011. An assessment of precipitation changes over Antarctica and the Southern Ocean since 1989 in contemporary global reanalyses. J. Clim. 24, 4189–4209. doi:10.1175/2011JCLI4074.1.

Calvert, D., Siddorn, J., 2013. Revised vertical mixing parameters for the UK community standard configuration of the global NEMO ocean model. Hadley Centre Technical Note 95.

Carsey, F.D., 1980. Microwave observation of the Weddell Polynya. Mon. Wea. Rev. 108, 2032–2044.

Chu, P.C., Fan, C., 2007. An inverse model for calculation of global volume transport from wind and hydrographic data. J. Mar. Sys. 65, 376–399.

Comiso, J.C., 2000. Bootstrap sea ice concentrations from Nimbus-7 SMMR and DMSP SSM/I-SSMIS. Version 2. Boulder, Colorado USA: NASA DAAC at the National Snow and Ice Data Center.

Comiso, J.C., Gordon, A.L., 1987. Recurring polynyas over the Cosmonaut Sea and the Maud Rise. J. Geophys. Res. 92 (C3), 2819–2833.

Cunningham, S.A., Alderson, S.G., King, B.A., Brandon, M., 2003. Transport and variability of the Antarctic Circumpolar Current in Drake Passage. J. Geophys. Res. 108 (C5). doi:10.1029/2001JC001147.

Dai, A., Qian, T., Trenberth, K.E., Milliman, J.D., 2009. Changes in continental freshwater discharge from 1948-2004. J. Clim. 22, 2773–2791.

Dee, D.P., Uppala, S.M., Simmons, A.J., co authors, 2011. The ERA-Interim reanalysis: configuration and performance of the data assimilation system. Q. J. R. Meteorol. Soc. 137 (656), 553–597. doi:10.1002/qj.828.

Doney, S.C., Hecht, M.W., 2002. Antarctic bottom water formation and deep-water chlorofluorocarbon distributions in a global ocean climate model. J. Phys. Oceanogr. 32, 1642–1666.

Döös, K., Nilsson, J., Nycander, J., Brodeau, L., Ballarotta, M., 2012. The world ocean thermohaline circulation. J. Phys. Oceanogr. 42, 1445–1460.

Gaspar, P., Grégoris, Y., Lefevre, J.-M., 1990. A simple eddy kinetic energy model for simulations of the oceanic vertical mixing: tests at station Papa and long-term upper ocean study site. J. Geophys. Res. 95 (C9), 16179–16193.

Gent, P.R., McWilliams, J.C., 1990. Isopycnal mixing in ocean circulation models. J. Phys. Oceanogr. 20, 150–155.

Goosse, H., Deleersnijder, E., Fichefet, T., England, M.H., 1999. Sensitivity of a global coupled ocean-sea ice model to the parameterization of vertical mixing. J. Geophys. Res. 104 (C6), 13681–13695.

Goosse, H., Fichefet, T., 2001. Open-convection convection and polynya formation in a large-scale ice-ocean model. Tellus 53A, 94–111.

Griffies, S.M., Gnanadesikan, A., Pacanowski, R.C., Larichev, V.D., Dukowicz, J.K., Smith, R.D., 1998. Isoneutral diffusion in a z-coordinate ocean model. J. Phys. Oceanogr. 28, 805–830.

Groeskamp, S., Zika, J.D., McDougall, T.J., Sloyan, B.M., Laliberté, F.B., 2014. The representation of ocean circulation and variability in thermodynamic coordinates. J. Phys. Oceanogr. 44, 1735–1750.

Haid, V., Timmermann, R., 2013. Simulated heat flux and sea ice production at coastal polynyas in the southwestern Weddell Sea. J. Geophys. Res. 118, 2640–2652. doi:10.1002/jgrc.20133.

Häkkinen, S., 1995. Seasonal simulation of the Southern Ocean coupled ice-ocean system. J. Geophys. Res. 100 (C11), 22733–22748.

Heuzé, C., Heywood, K.J., Stevens, D.P., Ridley, J.K., 2013. Southern Ocean bottom water characteristics in CMIP5 models. Geophys. Res. Lett. 40, 1409–1414. doi:10.1002/grl.50287.

Heuzé, C., Ridley, J.K., Calvert, D., Stevens, D.P., Heywood, K.J., 2015. Increasing vertical mixing to reduce Southern Ocean deep convection in NEMO. Geosci. Model Dev. Discuss. 8, 2949–2972. doi:10.5194/gmdd-8-2949-2015.

Holland, P.R., Bruneau, N., Enright, C., Losch, M., Kurtz, N.T., Kwok, R., 2014. Modeled trends in Antarctic sea ice thickness. J. Clim. 27, 3784–3801. doi:10.1175/JCLI-D-13-00301.1.

Hosking, J.S., Orr, A., Marshall, G.J., Turner, J., Phillips, T., 2013. The influence of the Amundsen–Bellingshausen seas low on the climate of west Antarctica and its representation in coupled climate model simulations. J. Clim. 26, 6633–6648. doi:10.1175/JCLI-D-12-00813.1.

Hunke, E.C., Lipscomb, W.H., Turner, A.K., Jeffrey, N., Elliott, S., 2013. CICE: the Los Alamos sea ice model documentation and software user's manual version 5.0. Los Alamos National Laboratory, Los Alamos NM Technical report. 87545

Jacobs, S.S., Giulivi, C.F., 2010. Large multidecadal salinity trends near the Pacific–Antarctic continental margin. J. Clim. 23, 4508–4524. doi:10.1175/2010JCLI3284.1.

Kurtz, N.T., Markus, T., 2012. Satellite observations of Antarctic sea ice thickness and volume. J. Geophys. Res. 117 (C08025). doi:10.1029/2012JC008141.

Legg, S., Hallberg, R.W., Girton, J.B., 2006. Comparison of entrainment in overflows simulated by z-coordinate, isopycnal and non-hydrostatic models. Ocean Model. 11, 69–97.

Liu, Y., Moore, J.C., Cheng, X., Gladstone, R.M., Bassis, J.N., Liu, H., Wen, J., Hui, F., 2015. Ocean-driven thinning enhances iceberg calving and retreat of Antarctic ice shelves. PNAS 112 (11), 3263–3268. doi:10.1073/pnas.1415137112.

Locarnini, R.A., Mishonov, A.V., Antonov, J.I., Boyer, T.P., Garcia, H.E., Baranova, O.K., Zweng, M.M., Paver, C.R., Reagan, J.R., Johnson, D.R., Hamilton, M., Seidov, D., 2013. World Ocean Atlas 2013, Volume 1: Temperature. In: Levitus, S., Mishonov, A. (Eds.). NOAA Atlas NESDIS 73.

Madec, G., 2014. NEMO ocean engine (Draft edition r5171). Institut Pierre-Simon Laplace (IPSL), France Technical report.

Madec, G., Imbard, M., 1996. A global ocean mesh to overcome the North Pole singularity. Clim. Dyn. 12 (6), 381–388. doi:10.1007/BF00211684.

Marsland, S., Wolff, J.-O., 2001. On the sensitivity of Southern Ocean sea ice to the surface freshwater flux: a model study. J. Geophys. Res. 106 (C2), 2723–2741.

Martin, T., Park, W., Latif, M., 2013. Multi-centennial variability controlled by Southern Ocean convection in the Kiel Climate Model. Clim. Dyn. 40, 2005–2022. doi:10.1007/s00382-012-1586-7.

Massonnet, F., Fichefet, T., Goosse, H., Vancoppenolle, M., Mathiot, P., Beatty, C.K., 2011. On the influence of model physics on simulations of Arctic and Antarctic sea ice. Cryosphere 5, 687–699. doi:10.5194/tc-5-687-2011.

Mathiot, P., Goosse, H., Fichefet, T., Barnier, B., Gallée, H., 2011. Modelling the seasonal variability of the Antarctic Slope Current. Ocean Sci. 7, 455–470. doi:10.5194/os-7-455-2011.

Megann, A., Storkey, D., Aksenov, Y., Alderson, S., Calvert, D., Graham, T., Hyder, P., Siddorn, J., Sinha, B., 2014. GO5.0: the joint NERC-Met Office NEMO global ocean model for use in coupled and forced applications. Geosci. Model Dev. 7, 1069–1092. doi:10.5194/gmd-7-1069-2014.

Meijers, A.J.S., 2014. The southern ocean in the coupled model intercomparison project phase 5. Phil. Trans. R. Soc. A. 372. doi:10.1098/rsta.2013.0296.

Rae, J.G.L., Hewitt, H., Keen, A., Ridley, J.K., Edwards, J., Harris, C., 2014. A sensitivity study of the sea ice simulation in the global coupled climate model, HadGEM3. Ocean Modell. 74, 60–76.

Rignot, E., Jacobs, S., Mouginot, J., Scheuchl, B., 2013. Ice-shelf melting around Antarctica. Science 341, 266–270. doi:10.1126/science.1235798.

Sallée, J.-B., Shuckburgh, E., Bruneau, N., Meijers, A.J.S., Bracegirdle, T.J., Wang, Z., 2013. Assessment of Southern Ocean mixed-layer depths in CMIP5 models: historical bias and forcing response. J. Geophys. Res. 118, 1845–1862. doi:10.1002/jgrc.20157.

Santoso, A., England, M.H., 2008. Antarctic bottom water variability in a coupled climate model. J. Phys. Oceanogr. 38, 1870–1893.

Silva, T.A.M., Bigg, G.R., Nicholls, K.W., 2006. Contribution of giant icebergs to the Southern Ocean freshwater flux. J. Geophys. Res. 111 (C03004). doi:10.1029/2004JC002843.

de Steur, L., Holland, D.M., Muench, R.D., McPhee, M., 2007. The warm-water "halo" around Maud Rise: properties, dynamics and impact. Deep-Sea Res. I 54, 871–896.

Stössel, A., Notz, D., Haumann, F.A., Haak, H., Jungclaus, J., Mikolajewicz, U., 2015. Controlling high-latitude Southern Ocean convection in climate models. Ocean Modell. 86, 58–75. doi:10.1016/j.ocemod.2014.11.008.

Stössel, A., Stössel, M.M., Kim, J.-T., 2007. High-resolution sea ice in long-term global ocean GCM integrations. Ocean Modell. 16, 206–223. doi:10.1016/j.ocemod.2006.10.001.

Timmermann, R., Beckmann, A., 2004. Parameterization of vertical mixing in the Weddell Sea. Ocean Modell. 6 (1), 83–100. doi:10.1016/S1463-5003(02)0061-6.

Timmermann, R., Beckmann, A., Hellmer, H., 2001. The role of sea ice in the fresh-water budget of the Weddell Sea, Antarctica. Ann. Glaciol. 33, 419–424.

Timmermann, R., Losch, M., 2005. Using the Mellor-Yamada mixing scheme in seasonally ice-covered seas - Corrigendum to: parameterization of vertical mixing in the Weddell Sea [Ocean Modelling 6 (2004) 83–100]. Ocean Modell. 10, 369–372.

Turner, A.J., Hunke, E.C., Bitz, C.M., 2013. Two modes of sea-ice gravity drainage: a parameterization for large-scale modeling. J. Geophys. Res. 118, 2279–2294. doi:10.1002/jgrc.20171.

Turner, J., Bracegirdle, T.J., Phillips, T., Marshall, G.J., Hosking, J.S., 2012. An initial assessment of Antarctic sea ice extent in the CMIP5 models. J. Clim. 26 (5), 1473–1484. doi:10.1175/JCLI-D-12-00068.1.

Uotila, P., Holland, P.R., Vihma, S., Marsland, T., Kimura, N., 2014. Is realistic Antarctic sea-ice extent in climate models the result of excessive ice drift? Ocean Modell. 79, 33–42. doi:10.1016/j.ocemod.2014.04.004.

Wang, C., Zhang, L., Lee, S.-K., Wu, L., Mechoso, C.R., 2014. A global perspective of CMIP5 climate model biases. Nat. Climate Change 4, 201–205. doi:10.1038/NCLIMATE2118.

Wang, Z., Meredith, M.P., 2008. Density-driven Southern Hemisphere subpolar gyres in coupled climate models. Geophys. Res. Lett. 35 (L14608). doi:10.1029/2008GL034344.

Worby, A.P., Geiger, C.A., Paget, M.J., Woert, M.L.V., Ackley, S.F., DeLiberty, T.L., 2008. Thickness distribution of Antarctic sea ice. J. Geophys. Res. 113 (C05S92). doi:10.1029/2007JC004254.

Zweng, M., Reagan, J., Antonov, J., Locarnini, R., Mishonov, A., Boyer, T., Garcia, H., Baranova, O., Johnson, D., Seidov, D., Biddle, M., 2013. World Ocean Atlas 2013, Volume 2: Salinity. In: Levitus, S., Mishonov, A. (Eds.). NOAA Atlas NESDIS 74. National Oceanographic Data Center, Silver Spring, MD, USA.